

Journal of Materials Chemistry B

Accepted Manuscript



This is an *Accepted Manuscript*, which has been through the Royal Society of Chemistry peer review process and has been accepted for publication.

Accepted Manuscripts are published online shortly after acceptance, before technical editing, formatting and proof reading. Using this free service, authors can make their results available to the community, in citable form, before we publish the edited article. We will replace this *Accepted Manuscript* with the edited and formatted *Advance Article* as soon as it is available.

You can find more information about *Accepted Manuscripts* in the [Information for Authors](#).

Please note that technical editing may introduce minor changes to the text and/or graphics, which may alter content. The journal's standard [Terms & Conditions](#) and the [Ethical guidelines](#) still apply. In no event shall the Royal Society of Chemistry be held responsible for any errors or omissions in this *Accepted Manuscript* or any consequences arising from the use of any information it contains.

ARTICLE

Amine end-functionalized poly(2-ethyl-2-oxazoline) as promising coating material for antifouling applications

Cite this: DOI: 10.1039/x0xx00000x

Received 00th January 2012,
Accepted 00th January 2012

DOI: 10.1039/x0xx00000x

www.rsc.org/

Lutz Tauhardt,^{a,b} Marion Frant,^c David Pretzel,^{a,b} Matthias Hartlieb,^{a,b} Christian Bücher,^c Gerhard Hildebrand,^c Bernd Schröter,^d Christine Weber,^{a,b} Kristian Kempe,^{a,b,†} Michael Gottschaldt,^{a,b} Klaus Liefeth^c and Ulrich S. Schubert^{*a,b,e}

The antifouling behavior of different poly(2-ethyl-2-oxazoline)s (PEtOx) coatings was investigated under “real live” conditions. Amine end-functionalized PEtOx of different molar masses have been prepared using a new and straight-forward, two step synthesis method. Subsequently, the PEtOx were attached to glass surfaces via a tetraether lipid and a common silane, respectively. The polymers and coatings were characterized using techniques such as ¹H NMR spectroscopy and MALDI-TOF-MS as well as XPS and contact angle measurements. In a next step, the coatings were exposed to the simultaneous attack of five different bacteria in synthetic river water. A clear reduction of the biofilm formation was observed. In addition, the stability of the coatings against thermal, mechanical, and chemical stress was studied.

Introduction

Preventing the uncontrolled adhesion and adsorption of proteins, cells, bacteria, and other microorganisms onto surfaces, the so called fouling process, represents a major challenge for a wide range of applications such as medicine (*e.g.* medical devices, implants, drug delivery systems),^{1, 2} mobility (*e.g.* ship hull coatings),^{3, 4} food industry (*e.g.* packaging),⁵ but also for membranes (*e.g.* in water purification systems),⁶ microarrays, and (bio)sensors.⁷

In principle one can distinguish between two types of antifouling coatings: (1) Bioactive coatings that cause a direct or indirect inactivation of adherent microorganisms or biofilms by either releasing an antifouling agent (*e.g.* biocides), or by killing the cells, bacteria, or microorganisms on contact using specific molecules (*e.g.* quarternized polymers), and (2) biopassive coatings, which reduce fouling due their protein and cell repellent character without interfering with the proliferation cycle or the cell metabolism.⁸⁻¹⁰ However, coatings that are bioactive or release antifouling agents suffer from a loss of activity over time. In case of bioactive coatings self-deactivation occurs due to the fact that dead cells or microorganisms adhere to the active layer, cover it and, therefore, allow the adhesion and proliferation of new cells on the cell debris.¹⁰ Coatings that release antifouling agents lose

their activity when all antifouling agent (*e.g.* biocide) is consumed. Moreover, they are harmful to the environment, since the released antifouling agents are not only active on the surface that should be protected and, hence, can kill in a nonselective way or accumulate in microorganism, animals (*e.g.* fish), and plants.^{11, 12} An approach to overcome these issues is the covalent binding of the antifouling coatings onto the surface. In particular biopassive coatings are promising, since they are not self-deactivating and do not release toxic and polluting compounds. Recently published studies have led to the conclusion that materials for biopassive coating have to meet the following criteria: (1) The presence of hydrogen bond accepting and hydrophilic (polar) groups, and (2) the absence of hydrogen bond donating groups and of net charges.^{8, 13} If we otherwise accept, that the formation of a hydration layer (water barrier) is a vital prerequisite to build up anti-adhesive surfaces with non-fouling properties hydrogen bond accepting groups are of the same importance than hydrogen bond donating groups.¹⁴ Based on the possibility to tune their properties, polymers can be adapted to a wide range of requirements and, thus, represent an interesting class of compounds for such surface tethered antifouling coatings. A widely used polymer for biopassive and repellent coatings is poly(ethylene glycol) (PEG).^{8, 15-18} However, PEG is known to undergo degradation

by (auto-)oxidation to form ethers and aldehydes, hampering its long-term application.^{13, 19-22} On this account, poly(2-oxazoline)s (POx), in particular the water soluble poly(2-methyl-2-oxazoline)s (PMeOx) and poly(2-ethyl-2-oxazoline)s (PEtOx), are investigated as alternative coating materials.^{13, 19, 23-31} Compared to the synthesis of PEG by anionic polymerization, the preparation of POx by cationic ring-opening polymerization (CROP) is less labor demanding, but also yields well-defined polymers with controlled molar masses and low polydispersity index (PDI) values. Moreover, a broad variety of functional electrophilic initiators, nucleophilic terminating agents, and 2-oxazoline monomers allow the synthesis of well-defined (co)polymers and the tuning of the polymer properties.³² It was shown that POx coatings have similar antifouling properties as PEG, but are stable in an oxidizing environment.^{13, 19} However, up to now all antifouling investigations on POx surfaces were performed under laboratory conditions using only a single type of protein (*e.g.* fibronectin,^{29, 30} bovine serum albumin^{27, 28}), cell (*e.g.* fibroblasts²⁴), or bacterium (*e.g.* *E. coli*^{13, 25, 26}). A review on methods to attach POx to surfaces as well the properties and applications of POx functionalized surfaces was published recently.³³

The chemical long-term stability of antifouling coatings is mandatory and can be greatly improved by covalent tethering of the polymers to the surface *via* linker molecules. Recently, tetraether lipids (TEL), *i.e.* bipolar membrane spanning lipids from thermoacidophilic archaea, were presented as an interesting new class of linker molecules.³⁴⁻³⁹ By a simple self-assembling process, a stable, highly ordered impermeable TEL monolayer (~4 nm) with biomembrane-like properties is formed. The covalent immobilization of this thin lipid layer on surfaces can be achieved easily when the lipid headgroups are functionalized with cyanuric chloride.^{35-37, 39} An outstanding property of TELs is their excellent stability against oxidation, acidic and basic hydrolysis as well as biodegradation, which is based on the fully saturated character of the methyl branched alkyl chains.³⁴ Moreover, biocompatibility analyses revealed that TELs are both nontoxic and immunologically inert and, additionally, exhibit antifouling activity.³⁵⁻³⁸ Hence, the usage of TEL linkers to attach POx to surfaces is highly interesting.

Here, we report the antifouling behavior of amine end-functionalized PEtOx, covalently bound to glass substrates using two different methods: (1) Attachment *via* the epoxide ring-opening reaction of a common glycidyl ether silane tethered to the surface as described in literature, *e.g.* for PEG,^{15, 40} and (2) immobilization *via* the cyanuric chloride functionalized headgroups of a TEL linker. To this end, a new approach to synthesize amine end-functionalized POx was developed. PEtOx of different chain lengths were prepared and characterized by ¹H NMR spectroscopy, matrix-assisted laser desorption/ionization time of flight laser mass spectrometry (MALDI-TOF-MS), and size exclusion chromatography (SEC). The PEtOx coatings were analyzed by contact angle measurements and X-ray photoelectron spectroscopy (XPS). The subsequent antifouling investigations were performed in

synthetic river water using a microbiological mixed culture consisting of five different types of bacteria. Biofilm formation and the stability of the coating were studied using confocal laser scanning microscopy.

Methods and materials

General methods and surface characterization

Used chemicals, instruments, and characterization methods are described in the supporting info.

Synthesis of phthalimide end-capped PEtOx (1)

A solution of initiator (MeOTs), monomer (EtOx), and solvent (acetonitrile) was prepared with a total monomer to initiator ratio of [M]/[I] = 20, 40, 60, and 80, respectively. The total monomer concentration was adjusted to 4 M. The solution was heated at 140 °C in a microwave synthesizer for a predetermined time. After cooling to room temperature a 2-fold excess of potassium phthalimide was added and the reaction mixture was stirred overnight at 70 °C. The reaction mixture was filtered and the solvent removed. The residue was dissolved in chloroform and washed twice with a saturated aqueous solution of NaHCO₃ and once with brine. The organic phase was dried over sodium sulfate. After filtration, the polymer was concentrated under reduced pressure, precipitated into ice-cold diethyl ether, and dried at 40 °C under reduced pressure.

Synthesis of amine end-capped PEtOx (2)

Phthalimide end-capped PEtOx was dissolved in ethanol and a 10-fold excess of hydrazine monohydrate was added. The reaction mixture was heated under reflux overnight. After cooling to room temperature, a concentrated hydrochloric acid was added to adjust the pH value to 2-3. The precipitate was removed by filtration and the ethanol was evaporated. The residue was dissolved in water and aqueous sodium hydroxide solution until pH value reached 9-10. The aqueous solution was extracted thrice with chloroform. The organic phase was dried over sodium sulfate, concentrated, and precipitated into ice-cold diethyl ether. The white precipitate was filtered off and dried at 40 °C under reduced pressure.

Synthesis of fluorescein labeled P(EtOx-*stat*-AmOx) (Fluo-PEtOx) (5)

The starting material P(EtOx₃₆-*stat*-AmOx₄) (4) was synthesized as reported earlier.⁴¹ P(EtOx₃₆-*stat*-AmOx₄) (1 g, 242 μmol) was dissolved in DMSO (50 mL). 5(6)-Carboxyfluorescein *N*-hydroxysuccinimide ester (114.5 mg, 242 μmol, 1 eq. per polymer chain) and TEA (2.5 mL) were added to the solution and the reaction was stirred for 3 h. Subsequently, the product was precipitated in

cold diethyl ether (700 mL), filtered off, dissolved in methanol (20 mL) and precipitated again into diethyl ether (200 mL). The polymer was obtained as orange solid (1.039 g, 95%).

Coating procedure for silane on borofloat® 33 glass slides

Prior to use, each side of the glass slides was cleaned in oxygen plasma for 15 min. In a glove box, the glass slides were treated with (3-glycidyloxypropyl)trimethoxysilane for 1 h and subsequently rinsed with dry DMF. One side of the glass slide was covered with the respective polymer solution in DMF (200 mg/mL) at a concentration of 3 mL/cm² (64 mg/cm²). Then, a second glass slide was put on top (face-to-face assembly). After 2 days at room temperature, the slides were separated, intensely rinsed with deionized water and air-dried.

Coating procedure for tetraether lipid on borofloat® 33 glass slides

Preparation of TEL vesicle emulsion:

The main phospholipid included in dried biomass of *Sulfolobus acidocaldarius* was isolated and purified as described earlier.³⁹ The head-groups of the extracted tetraether lipid were activated by refluxing with cyanuric chloride over 1 week in dry chloroform/methanol (1:1).

The activated lipids were dissolved in dry chloroform/methanol 1:1, sodium bicarbonate (1.5 g per 100 mg lipid) was added and a thin lipid layer at the sides of the flask was formed. Subsequently, the solvents were removed completely under reduced pressure. The lipid film was hydrated with pure water at a final lipid concentration of about 2 mg/mL. Further treatment in an ultrasonic bath at 50 °C for 15 minutes yielded a cloudy lipid emulsion consisting of large multilamellar vesicles. Afterwards, the emulsion was extruded through a polycarbonate membrane (pore diameter 100 nm).

Coating:

The glass substrates were purified as follows: (1) Sonication in diluted detergent solution (Blanchipon®, Optical II), (2) incubation in ethanol and 35% nitric acid, and (3) storing in de-ionised water. Subsequently, the surfaces were activated with nitric acid and by exposure to UV irradiation. After amino silanization using 3-(ethoxydimethylsilyl)propylamine the substrates were cleaned with chloroform, methanol, and water. TEL coating was performed *via* liposome spreading in a PTFE reaction chamber by incubation with a freshly prepared lipid emulsion at 70 °C overnight.³⁹ Finally, the coated substrates were sonicated in chloroform for 10 minutes and dried with pressurized air. In a next step, the PEtOx were immobilized on the TEL-coated glass by coupling the amine end group of the polymer with the cyanuric chloride moiety of the TEL. The reaction was performed in borate buffer solution (10 mg PEtOx/mL, pH = 8.5) at 60 °C overnight. Subsequently, the glass slides were extensively rinsed with distilled water and dried under ambient conditions.

Preparation of synthetic river water medium

The synthetic river water was prepared by dissolving calcium chloride dihydrate (34.6 mg/L), magnesium sulfate heptahydrate (112.3 mg/L), sodium bicarbonate (126.0 mg/L), monopotassium phosphate (4.35 mg/L), sodium nitrate (85.0 mg/L), glucose (6.6 mg/L), and pepton (2.0 mg/L) in distilled water.

Five typical microorganisms with a high potential of biofilm formation were isolated from the river Ruhr near Mühlheim (Germany): *Aeromonas hydrophila/caviae*, *Sphingomonas paucimobilis*, *Pasteurella spp.*, *Aeromonas salmonicida*, and *Leuconostoc spp.*. The microorganisms were precultivated at 30 °C overnight on a shaker (100 rpm) in a special water medium (pH 7) consisting of: yeast extract (0.5 g/mL), peptone (0.5 mg/mL), casein hydrolysate (0.5 mg/mL), glucose (0.5 mg/mL), sodium pyruvate (0.3 mg/mL), starch (0.5 mg/mL), dipotassium hydrogenphosphate (0.3 mg/mL), and monopotassium phosphate (0.05 mg/mL). Bacteria were harvested by centrifugation at 4,000 g for 15 min. The pellet was washed twice with synthetic river medium to remove other particle-like components that may have an impact on the kinetic process. A constant cell concentration of 2×10^6 cells/mL synthetic river water was adjusted.

Investigation of the biofilm formation

Polymer coated sterilized glass slides were incubated in flow chambers. Prior to use, all probes were sterilized using ethanol (70%). Subsequently, the coated glass slides were placed in a flow chamber running with bacteria containing synthetic river water at a flow rate of 0.3 mL/min at room temperature. After incubating for 15 hours, a rinsing cycle with pure cultivation medium was performed to remove non-adhered microorganisms from the surface. The bioadhesion was evaluated by means of confocal laser scanning microscopy. To this end, the adherent microorganisms were stained using a LIVE/DEAD® BacLight™ Bacterial Viability Kit (Molecular Probes, Germany). At each sample ten images of biofilms were taken at different positions in the flow channel by confocal laser scanning microscopy (LSM710, Zeiss microscopy, Germany, Plan Apochromat 5×/0.16). The surface area covered by microorganisms was quantified by software supported analysis of the microscopy images (Volocity improvisation®). Bioadhesion experiments were performed in triplicate.

Stability tests

Stability test were performed on Fluo-PEtOx coated glass slides attached *via* TEL and silane linker, respectively.

Investigation of the resistance against chemical stress:

Samples were incubated at room temperature over 12 weeks in an upright position in closed boxes on a shaker (75 rpm) filled with sterile filtrated water of a drinking water dam

(Neustadt/Ilm, Germany) and salt water from the North sea, respectively. Media were changed weekly.

Investigation of the resistance against mechanical stress:

Resistance against mechanical stress was investigated using aluminum oxide and silicon carbide particles in distilled water, based on environmental data. The test solution comprised 150 mg particles per liter. The particle size was distributed as follows: \varnothing 320 μm = 0.4%, \varnothing 120 μm = 41%, \varnothing 20 μm = 31.8%, \varnothing 9 μm = 26.8%. Samples were incubated at room temperature in a closed beaker glass with stirring (750 rpm) corresponding to a streaming of 2 m/s. Over 1 week a permanent change between 8 h rotation time and 16 h resting time without rotation was realized.

Investigation of the resistance against thermal stress:

In order to investigate thermal stability the samples were placed in distilled water and exposed to a defined temperature protocol with 25 cycles between 2 and 38 °C and an incubation period of 14 d. Dwell time at each temperature was 1 h.

Image analysis:

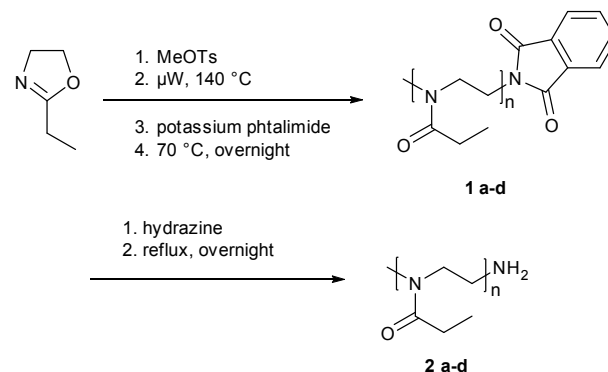
After each stress procedure fluorescence image data of the Fluo-PEtOx coated samples were recorded by confocal laser scanning microscopic method (LSM710, Zeiss microscopy, Germany, Plan Apochromat 5 \times /0.16). The recordings were made with uniform measurement parameters (gain, offset, pinhole, average, etc.) to allow a comparison of results among each other but also to untreated coatings as a proof of the layer stability.

Results and discussion

Synthesis and characterization of amine end-capped poly(2-ethyl-2-oxazoline)s

PEtOx of different molar masses were prepared with the aim to covalently bind the polymer to the surface *via* an epoxide bearing silane or a cyanuric chloride functionalized tetraether lipid (TEL), respectively. Since it is known that both epoxides and cyanuric chloride can react quite easily with amines, PEtOx bearing an amine end group were prepared using a new synthetic route.

The synthesis of an amine end-functionalized poly(2-oxazoline) (POx) was already described in literature. Lin *et al.* terminated the living oxazolinium species directly with ammonia in acetonitrile.⁴² However, the authors only obtained a degree of functionalization of about 80%. As an alternative three step method, Park *et al.* quenched the reaction mixture with a methanolic NaOH solution.⁴³ The resulting hydroxyl end group was then reacted with phthalimide in the presence of triphenylphosphine and diethyl azodicarboxylate to yield a POx with a phthalimide end group. In a final step, the amine end group was obtained by treatment with hydrazine monohydrate. However, this procedure led only to an amine end group



Scheme 1 Schematic representation of the synthesis of amine end-functionalized PEtOx.

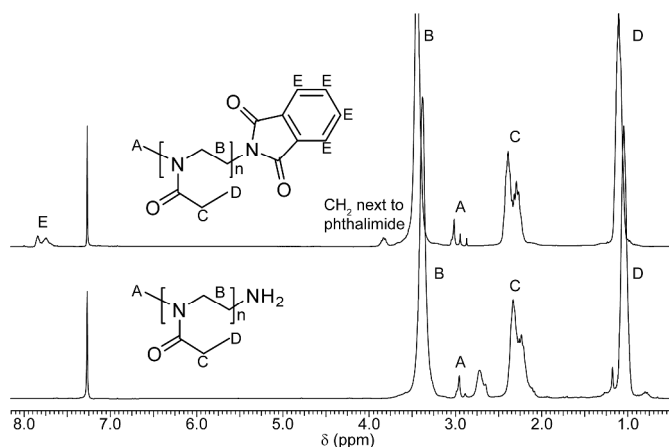


Fig. 1 ^1H NMR spectra of phthalimide (1a, top) and amine (2a, bottom) end-functionalized PEtOx (300 MHz, solvent CDCl_3).

functionalization efficiency of 62%. An additional problem, reducing the efficiency of this method, is the possible formation of ester end groups instead of hydroxyl end groups, when the reaction is quenched.⁴⁴⁻⁴⁶ These esters need to be hydrolyzed to hydroxyl groups before the polymer can be further functionalized. To overcome the drawbacks of these methods, a new synthetic route to synthesize amine end functionalized PEtOx was developed (Scheme 1). In this approach the living cationic species is quenched directly with an excess of potassium phthalimide, saving on step compared to the method described by Park *et al.* Moreover, the end-capping efficiency is quantitative according to ^1H NMR spectroscopy and MALDI-TOF-MS.

The ^1H NMR spectrum of **1** (Fig. 1 top) shows a broad signal around 7.76 ppm deriving from the aromatic protons of the phthalimide unit (4 protons). By correlation with the signals at about 3 ppm, which are associated with the CH_3 α -end group (3 protons), the quantitative functionalization with the desired ω -end group is confirmed. The broad peak at 3.44 ppm derives from the polymer backbone. The side chain signals can be found at 1.11 ppm (CH_3) and 2.32 ppm (CH_2), respectively.

Due to a different chemical environment, the back bone CH₂ group adjacent to the phthalimide is shifted to 3.83 ppm.

The MALDI-TOF mass spectrum of **1** shows two distributions that can be assigned to the sodium adduct of phthalimide end-capped PETox (Fig. 2). The methyl-initiated species derives from the initiation of the polymerization with methyl tosylate. The proton-initiated species is formed by chain transfer reactions occurring during the polymerization.^{47, 48} A hydroxyl end group bearing species could not be observed. This fact further underlines the complete functionalization and is in accordance with the results from ¹H NMR analysis. Moreover, the measured isotopic patterns match with the calculated isotopic patterns of the assigned species.

The phthalimide end-capped PETox **1** were subsequently treated with hydrazine monohydrate to obtain the amine functionalized polymers (**2**).^{43, 49} Characterization of the product by ¹H NMR spectrometry reveals the success of the reaction (Fig. 1 bottom). After the hydrazinolysis, the signals of the aromatic phthalimide end group and the CH₂ group adjacent to the phthalimide disappeared quantitatively.

The MALDI-TOF mass spectrum of **2** shows two major distributions which belong to the sodium adducts of methyl and

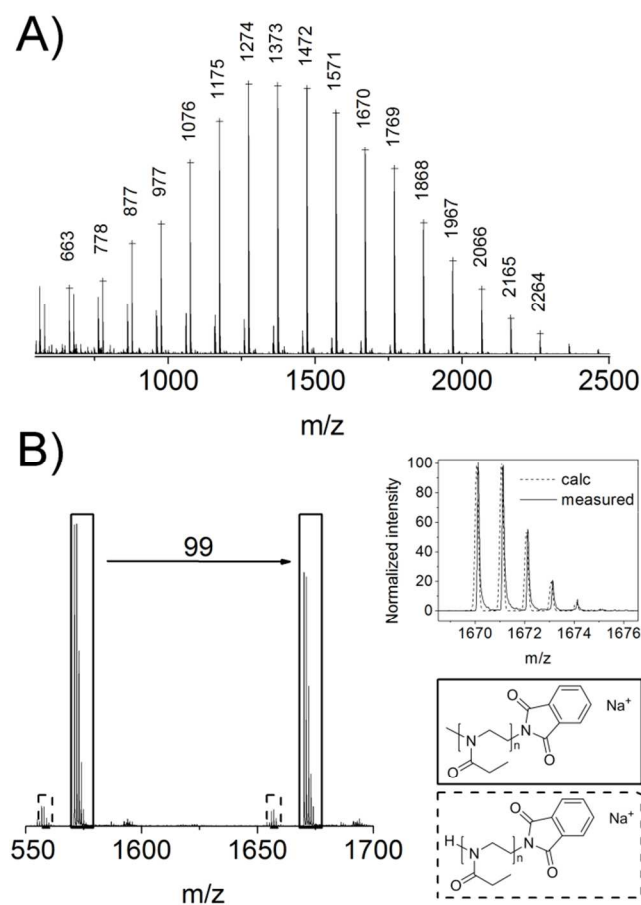


Fig. 2 MALDI-TOF mass spectrum of phthalimide end-capped PETox (left), an expanded region of the spectrum (right), the structural assignments for the different distributions as well as the calculated and measured isotopic pattern of the peak at $m/z = 1670$.

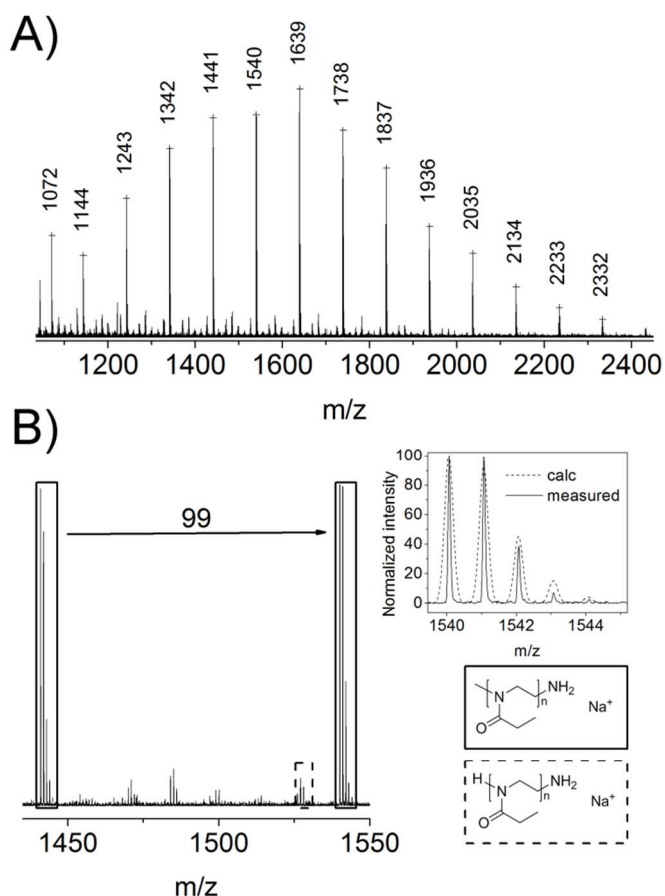


Fig. 3 MALDI-TOF mass spectrum of amine functionalized PETox (left), an expanded region of the spectrum (right), the structural assignments for the different distributions as well as the calculated and measured isotopic pattern of the peak at $m/z = 1540$.

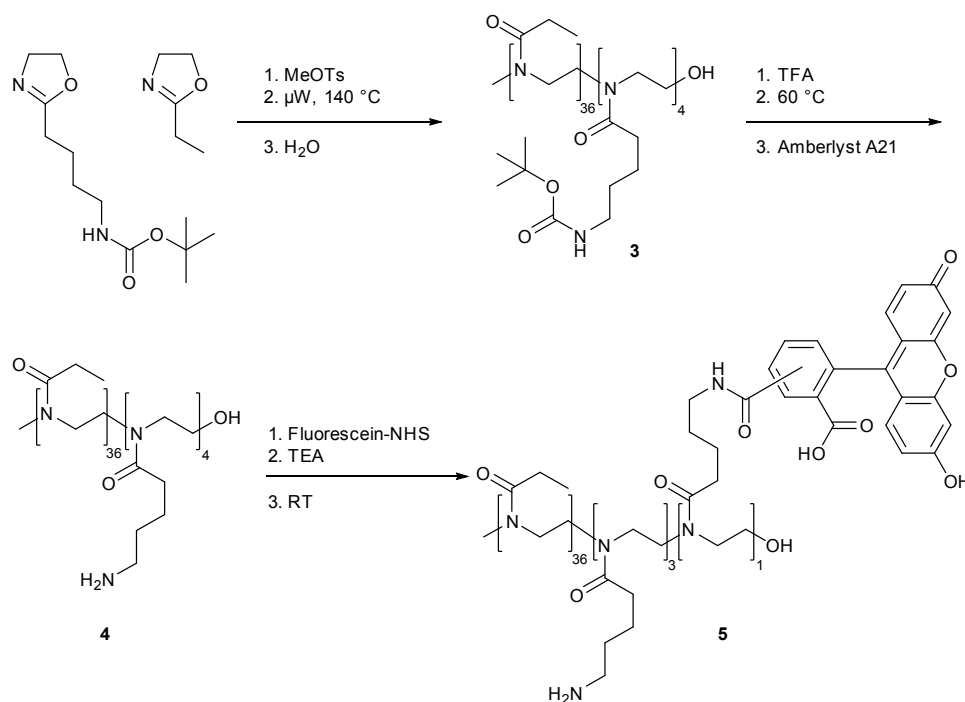
proton initiated PETox bearing an amine end group (Fig. 3). The initial phthalimide-bearing species could not be detected anymore. In addition, the measured and the calculated isotopic pattern coincide.

The presented synthesis route was used to prepare amine functionalized PETox (**2**) with different of molar masses, namely 2,000, 4,000, 6,000, and 8,000 g/mol ($n = 20, 40, 60$), which can be achieved simply by variation of the $[M]/[I]$ ratio applied for the CROP. Characterization by size exclusion chromatography (SEC) revealed PDI values between 1.12 and 1.19 (Table 1).

Table 1 SEC-Data of the different POx.

Sample	EtOx:BocOx:AmOx:F	M_n (g/mol) ^{a)}	PDI ^{a)}
2a	20:0:0:0	2,460	1.12
2b	40:0:0:0	3,790	1.15
2c	60:0:0:0	5,175	1.14
2d	80:0:0:0	5,990	1.19
3	36:4:0:0	5,300	1.08
4	36:0:4:0	5,400	1.12
5	36:0:3:1	5,500	1.18

^{a)} Determined by SEC (eluent: CHCl₃/2-propanol/TEA, calibration with a PS standard)



Scheme 2 Schematic representation of the synthesis of amine containing POx and labeling of the polymer with fluorescein.

Fluorescein labeled PEtOx

To prove the suitability of the attachment methods and to investigate the stability of the obtained PEtOx layers against different types of stress, a fluorescein labeled PEtOx (Fluo-PEtOx, **5**) was used. To this end, a copolymer with an amine content of 10% and an overall degree of polymerization (DP) of 40 ($P(\text{EtOx}_{36}\text{-stat-AmOx}_4)$, **4**) was synthesized by copolymerization of EtOx and a *tert*-butyloxycarbonyl (Boc)-protected amine group containing 2-oxazoline followed by deprotection (Scheme 2).⁴¹ In a next step one amine group was labeled using a fluorescein-NHS ester derivative. The reaction of this activated acid with amine groups is highly efficient under basic conditions and was, therefore, performed with triethylamine (TEA) as a base. Purification was accomplished by repeated precipitation into diethyl ether to eliminate traces of unreacted fluorescein. The successful labeling of the copolymer was confirmed by SEC, which provided congruent UV (485 nm) and RI-detector traces (Table 1, Fig. S1). Moreover, no signal of unreacted fluorescein was detected. In addition, ¹H NMR spectroscopy shows the characteristic peaks of fluorescein with broadening attributed to the attachment to the polymer chain (Fig. S2).

Coating of glass slides with PEtOx of different molar masses using different spacers

To investigate their suitability for the prevention of bioadhesion, the PEtOx polymers (**2a-d**) were immobilized on borofloat[®] 33 glass employing either 1) a silane based linker or 2) a TEL linker (Scheme 3). In case of coupling *via* a silane

based linker, the glass slides were first treated with (3-glycidyloxypropyl)trimethoxysilane (GOPTMS). Subsequently, PEtOx of different molar masses were attached by reaction of the epoxide unit of GOPTMS with the end group of the polymer (Scheme 3A route 1). For the coupling *via* a TEL linker (Scheme 3B) the terminal hydroxyl groups of the lipid were modified with cyanuric chloride to enable the covalent coupling to the glass surfaces as well as the covalent binding of PEtOx on top of the lipid membrane (Scheme 3A route 2). The TEL functionalized glass slides were coated with PEtOx with the same molar masses as for route 1.

Characterization of the polymer thin films

In order to examine the suitability of the attachment methods and the quality of the PEtOx coatings, fluorescein labeled PEtOx was grafted to the different linker molecules in the same way as the PEtOx homopolymers. By means of laser scanning microscopy it could be shown that homogenous Fluo-PEtOx films are obtained for both the GOPTMS and the TEL linker (Fig. 4).

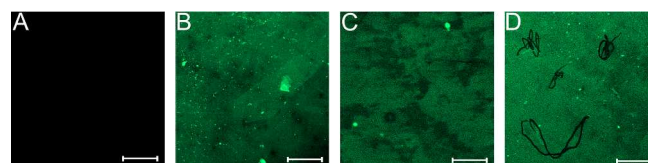
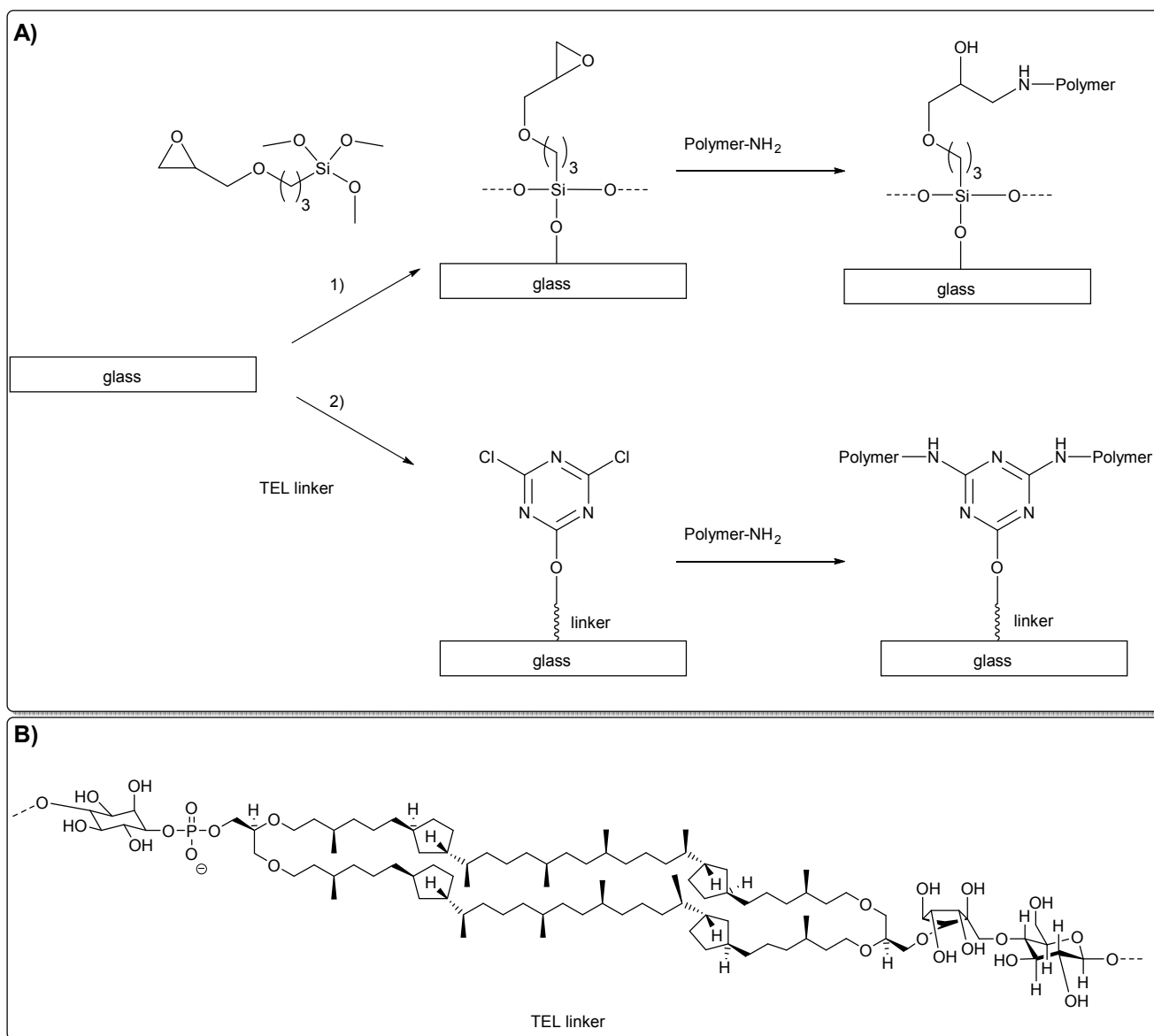


Fig. 4 Fluorescence microscope images of A) uncoated glass, B) Fluo-PEtOx attached *via* GOPTMS, C) Fluo-PEtOx attached *via* TEL, and D) scratched sample of Fluo-PEtOx attached *via* GOPTMS (scale bar: 100 μ m).



Scheme 3 A) Schematic representation of the PETox coating process using GOPTMS (route 1) and a TEL (route 2) linker, respectively, and B) of the TEL linker.

The coating process with the PETox homopolymers was further monitored by means of X-ray photoelectron spectroscopy (XPS). Using this method information on the chemical composition of surface layers, which are only a couple of nanometers thick, can be obtained. A comparison of the nitrogen 1s signal of pure borofloat glass, the different linkers, and the different PETox films showed the successful coating (Fig. 5). While on pure glass and GOPTMS treated substrate, no nitrogen was found, the TEL coated glass shows a nitrogen signal due the cyanuric chloride moieties. Moreover, the nitrogen signal intensity increased significantly after attaching the PETox.

Water contact angle measurements on air-dried and hydrated polymer coatings were performed with the aim to investigate the wetting behavior of the surface tethered PETox films (Fig. 6). Both, samples that were coated with GOPTMS and TEL

linker, respectively, displayed an increased water contact angle compared to the reference borosilicate glass (after treatment with argon plasma). Subsequent PETox grafting further increased the water contact angles for GOPTMS attached samples. In case of TEL linked PETox only for a DP of 20, referred to as 20(TEL), an increasing contact angle could be observed when compared to pure TEL. For all other chain lengths the contact angle is in the same range as for pure TEL or even decreased. These changes in wettability indicate a successful coating of the substrates with the linkers and PETox, respectively.

In the air-dried state, surfaces that were coated with PETox via a GOPTMS linker display water contact angles in a rather wide range between 57° and 85°. The variations for surfaces that were coated with PETox via TEL linkers are narrower, ranging from 53° to 70°. While for coatings attached through TEL

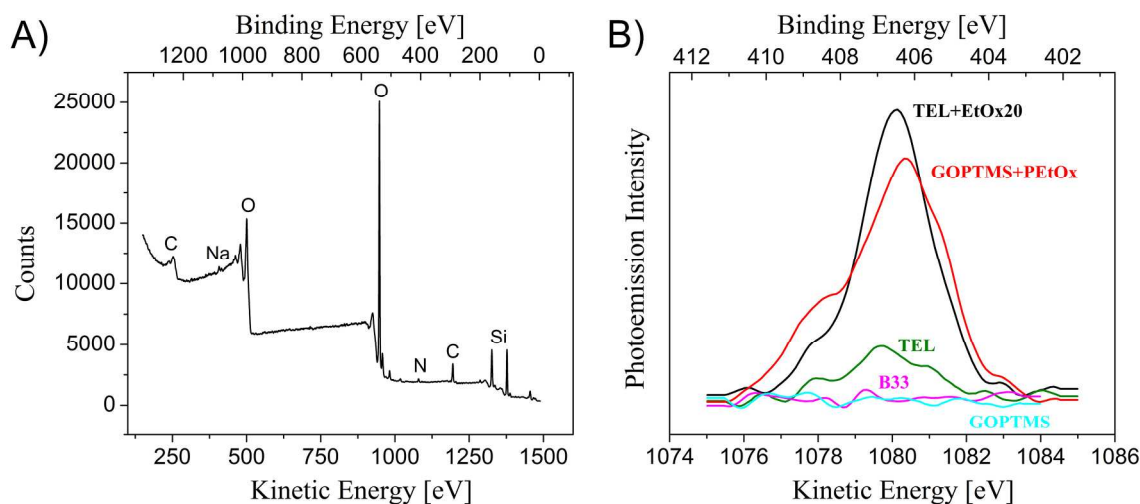


Fig. 5 A) Typical XPS spectrum of a TEL-PETox coating. B) Overlay of the nitrogen 1s signals of bare borofloat glass as well as the different linkers and coatings.

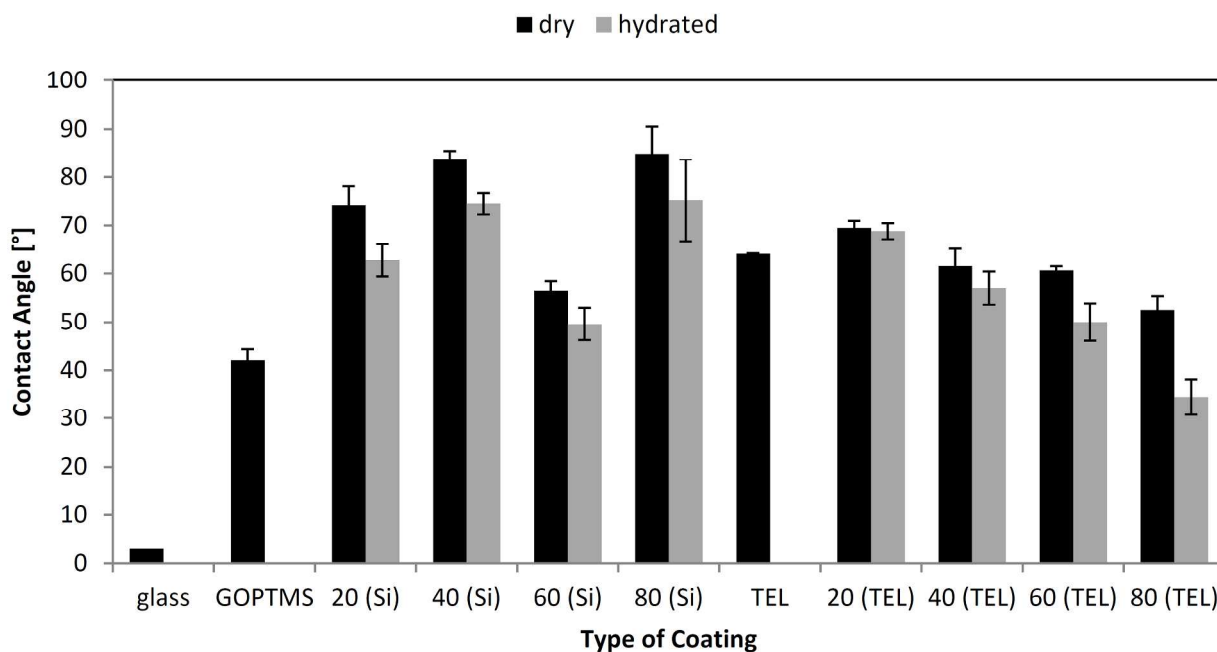


Fig. 6 Water contact angles of the different PETox-coatings in dry and hydrated state (data are presented as mean \pm standard deviation for $n = 45$). The numbers indicate the different DPs of PETox (20, 40, 60 and 80), linkers are given in brackets.

decreasing contact angles with increasing chain lengths could be observed, no trend could be found for GOPTMS attached PETox.

After swelling in water, the coatings display reduced contact angles. This finding is ascribed to the hydration of the hygroscopic, hydrophilic PETox. Again a clear trend to reduced contact angles for longer polymer chains can be found for TEL attached coatings. Moreover, the difference in contact angles between air-dried and hydrated state ($\Delta\theta$) increases with the chain length from 0.7° for $n = 20(\text{TEL})$ to 18.1° for $n = 80(\text{TEL})$. This observation indicates that longer polymers can

bind/absorb more water molecules and, thus, should have a higher antifouling potential. This is in accordance with theoretical calculation for PEG.⁸ For GOPTMS tethered films such tendency could not be observed. Here, a constant $\Delta\theta$ of $\sim 10^\circ$ was determined.

An important parameter with regard to the antifouling properties is the grafting density,³³ which is in general calculated either from the film thickness^{28, 50} or the weight loss of the sample upon heating.^{51, 52} However, due to technical reasons (*e.g.* monolayer, glass substrate) the determination of these parameters was not possible. To ensure the highest

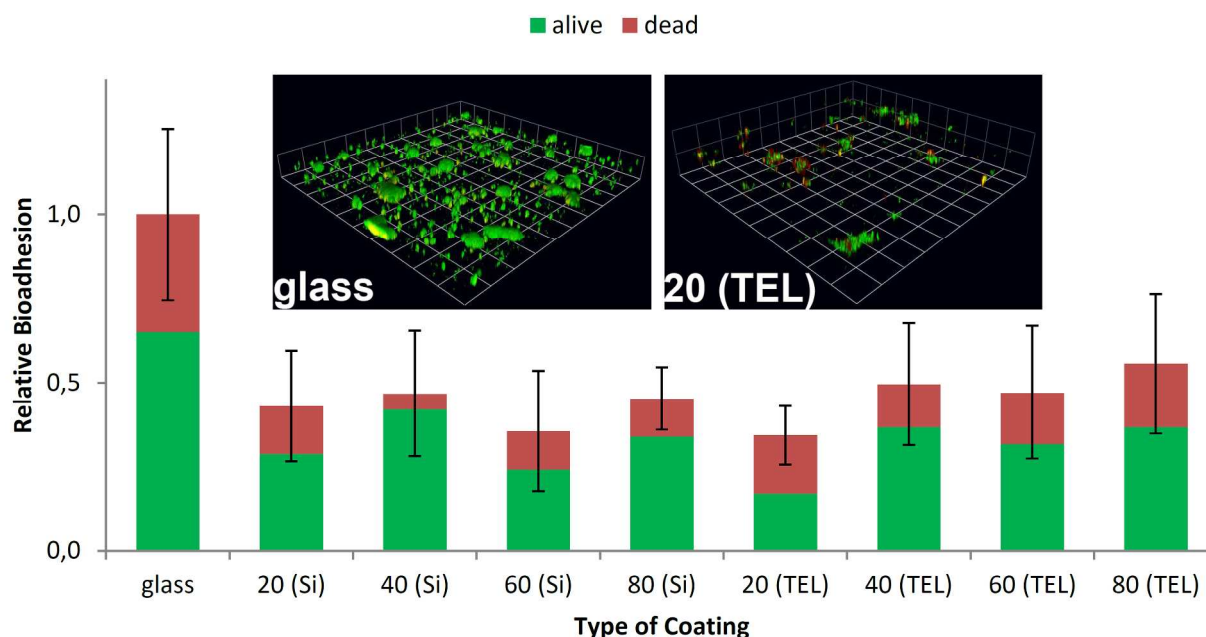


Fig. 7 Bioadhesion on PETox coatings of different DP (20, 40, 60, and 80) to the glass slides via a silane (Si) and a tetraether lipid (TEL) linker (standard deviation is related to the total bioadhesion (sum of dead and vital bacteria)) as well as laser scanning microscope images of the stained biofilms on glass and 20 (TEL).

Possible grafting density and excess of polymer was used.

Antifouling properties of the different PETox coatings

The antifouling properties of the different PETox-coated glass slides were investigated in flow-through chambers that allow a continuous cross flow of synthetic river water under reproducible conditions over an arbitrary period of time. Based on the water composition of the river Ruhr near Mühlheim (Germany), five different microorganisms with a high potential of biofilm formation were chosen, namely: *Aeromonas hydrophila/caviae*, *Sphingomonas paucimobilis*, *Pasteurella spp.*, *Aeromonas salmonicida*, and *Leuconostoc spp.*. After 15 hours incubation the adherent microorganisms were stained using a LIVE/DEAD[®] BacLight[™] Bacterial Viability Kit and investigated by means of confocal laser scanning microscopy. A clear reduction of the bioadhesion, induced by the PETox coatings, was detected (up to 66% compared to uncoated glass), with no significant differences between films attached via GOPTMS and TEL, respectively, suggesting that similar grafting efficiencies are reached (Fig. 7). Although in case of TEL linkers the hydrophilicity of swollen PETox samples increased with the chain length and longer chains should, therefore, have a higher antifouling potential, an influence of the molar mass on the cell adhesion could not be observed. Also the bacterial viability rate was hardly affected. Only the samples 40(Si) and 20(TEL) showed higher deviations. While on 40(Si) nearly no dead cells could be found, the 20(TEL) coating showed a reduced cell viability. In addition, 20(TEL) shows the lowest overall bioadhesion, making it the best coating produced within this study. However, from an use-

oriented point of view, *i.e.* for large scale applications, the attachment via GOPTMS is favored, since similar results are obtained and the coating process is easier. Moreover, GOPTMS, in contrast to TEL, is easily available in large amounts.

Antifouling properties of immobilized PEG- and POx-based coatings have been widely reported in the literature.^{8, 14-20} Due to the different, more real life test conditions, *e.g.* attack of multiple bacteria and synthetic river water medium, a comparison of the obtained results to other POx or PEG coatings, reported in literature, is difficult.

Stability of the PETox coatings

An important parameter with regard to their application, *e.g.* as sensor coatings, is the stability of the PETox films. To this end, Fluo-PETox coated glass slides, attached through GOPTS and TEL spacer, respectively, were exposed to three different types of stress: (1) chemical stress, (2) mechanical stress and (3) thermal stress. The resistance against chemical stress, caused *e.g.* by fresh and salt water, was investigated over 12 weeks using dam and North Sea water, respectively. The durability of the coatings against abrasion in particle containing water is essential in the field of environmental monitoring. Based on environmental data a corresponding test solution containing aluminum oxide and silicon carbide particles was prepared. Mechanical stress was simulated by placing the glass slides into this solution and stirring for 8 hours a day over 1 week. In order to verify their thermal stability, the samples were exposed to a defined heating profile for 14 days with temperatures between 2 and 38 °C. Subsequent analysis by means of confocal laser

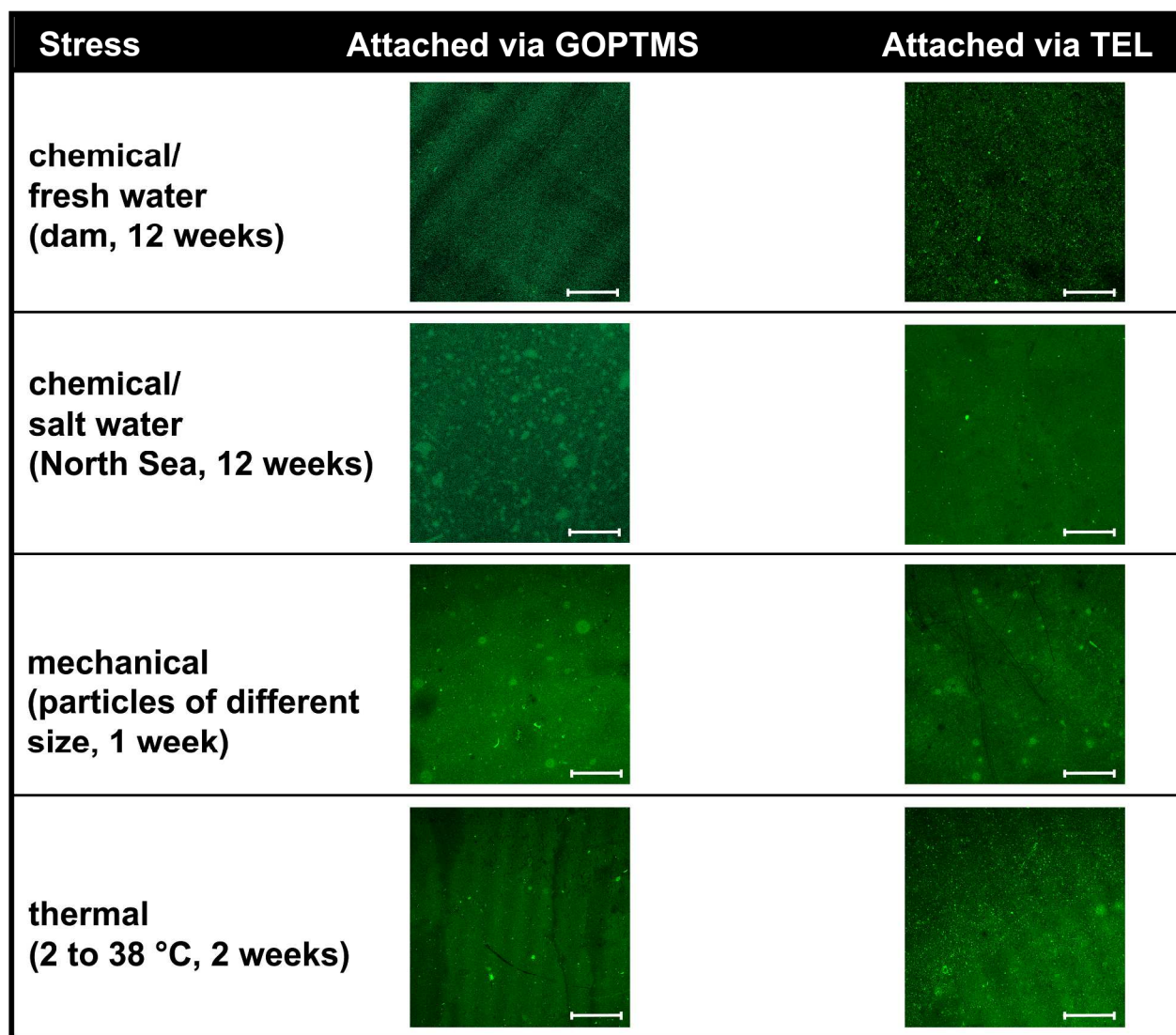


Fig. 8 Confocal laser scanning microscopy images of the Fluo-PEtOx coatings after stress tests (scale bar: 100 μ m).

scanning microscopy showed that the coatings withstood the different types of stress (Fig. 8).

Conclusion

The potential of PEtOx coatings to prevent bioadhesion under "real life" conditions was investigated. To this end, amine end-functionalized PEtOx of four different molar masses have been prepared applying a new and straightforward synthesis method. The polymers obtained were characterized by MALDI-TOF mass spectrometry, ^1H NMR spectroscopy, and size exclusion chromatography, which showed the successful introduction of ω -amine groups. PEtOx were attached to glass surfaces through silane and tetraether lipid based linkers. The surface immobilization of PEtOx was investigated by fluorescence microscopy measurements of surfaces modified with fluorescently labeled PEtOx as well as by XPS investigations,

which showed the presence of nitrogen signals after the PEtOx coating process. Contact angle measurements of air-dried and swollen coatings revealed a higher hydrophilicity of the swollen samples, ascribed to the formation of PEtOx hydrates. Fouling studies were performed in a flow-through chamber under "real-life" relevant conditions using a synthetic river water model containing five different bacteria. PEtOx modified glass samples exposed to the synthetic river water for 15 h showed a bioadhesion reduction of up to 66% with no significant differences between the two different linkers. The best results were obtained by PEtOx with 20 repeating units attached *via* a tetraether lipid linker, which revealed the lowest biofilm formation and the highest amount of dead bacteria. In addition, the stability of the PEtOx coatings towards chemical, mechanical, and thermal stress was investigated. No significant destruction of the polymer layer was observed, demonstrating the capability of the films for long term applications.

The present study underlines the potential of POx for antifouling coatings and is in agreement with other studies.³³ However, at the chosen, more realistic conditions, a complete reduction of biofilm formation could not be observed. Further investigations have to be performed and will aim at the application of mixtures of PEtOx with different molar masses as well as PEtOx of different architectures to result in a denser packing of the polymer chains on the surface. Another interesting aspect is probably the grafting of polyhydrophilic and polyzwitterionic entities to form a stable superficial water barrier. Future tests will have to show whether the presented coatings are able to maintain their antifouling behavior under real life conditions, *i.e.* the simultaneous acting of bacteria and stresses.

Acknowledgment

The authors would like to thank the Bundesministerium für Bildung und Forschung (Germany) funding (project: BASIS, 03WKCB01C) and 4H Jena Engineering for the stability tests. CW acknowledges the Carl-Zeiss foundation. KK is grateful to the Alexander von Humboldt-foundation for financial support.

Notes and references

^a Laboratory of Organic and Macromolecular Chemistry (IOMC), Friedrich Schiller University Jena, Humboldtstr. 10, 07743 Jena, Germany.

^b Jena Center for Soft Matter (JCSM), Friedrich Schiller University Jena, Philosophenweg 7, 07743 Jena, Germany.

^c Institute for Bioprocessing and Analytical Measurement Techniques e.V. (IBA), Rosenhof, 37308 Heilbad Heiligenstadt, Germany.

^d Institute for Solid State Physics, Friedrich Schiller University Jena, Helmholtzweg 5, 07743 Jena.

^e Dutch Polymer Institute (DPI), John F. Kennedylaan 2, 5612 AB Eindhoven, The Netherlands.

Corresponding author footnote: Fax. +49 3641 948 202; Email: ulrich.schubert@uni-jena.de

† Current address: Department of Chemical and Biomolecular Engineering, The University of Melbourne, Victoria 3010, Australia.

Electronic Supplementary Information (ESI) available: [details of any supplementary information available should be included here]. See DOI: 10.1039/b000000x/

- 1 V. K. Vendra, L. Wu and S. Krishnan, in *Nanotechnologies for the Life Sciences*, Wiley-VCH Verlag GmbH & Co. KGaA, 2007.
- 2 C. Blaszykowski, S. Sheikh and M. Thompson, *Chem. Soc. Rev.*, 2012, **41**, 5599-5612.
- 3 S. Cao, J. Wang, H. Chen and D. Chen, *Chin. Sci. Bull.*, 2011, **56**, 598-612.
- 4 P. Buskens, M. Wouters, C. Rentrop and Z. Vroon, *J. Coat. Technol. Res.*, 2013, **10**, 29-36.
- 5 T. Mérian and J. M. Goddard, *J. Agric. Food Chem.*, 2012, **60**, 2943-2957.
- 6 D. Rana and T. Matsuura, *Chem. Rev.*, 2010, **110**, 2448-2471.
- 7 C. Zhao, L.-Y. Li, M.-M. Guo and J. Zheng, *Chem. Pap.*, 2012, **66**, 323-339.
- 8 I. Banerjee, R. C. Pangule and R. S. Kane, *Adv. Mater.*, 2011, **23**, 690-718.
- 9 M. Charnley, M. Textor and C. Acikgoz, *React. Funct. Polym.*, 2011, **71**, 329-334.
- 10 F. Siedenbiedel and J. C. Tiller, *Polymers*, 2012, **4**, 46-71.
- 11 F. A. Guardiola, A. Cuesta, J. Meseguer and M. A. Esteban, *Int. J. Mol. Sci.*, 2012, **13**, 1541-1560.
- 12 J.-P. Maréchal and C. Hellio, *Int. J. Mol. Sci.*, 2009, **10**, 4623-4637.
- 13 R. Konradi, C. Acikgoz and M. Textor, *Macromol. Rapid Commun.*, 2012, **33**, 1663-1676.
- 14 K. Liefeth, H. Rothe, M. Frant and R. Schade, in *Biofunctional Surface Engineering*, ed. M. Scholz, Pan Stanford Publishing Pte. Ltd, Singapore, 2014, pp. 71-120.
- 15 J. Blümmel, N. Perschmann, D. Aydin, J. Drinjakovic, T. Surrey, M. Lopez-Garcia, H. Kessler and J. P. Spatz, *Biomaterials*, 2007, **28**, 4739-4747.
- 16 A. Rosenhahn, S. Schilp, H. J. Kreuzer and M. Grunze, *Phys. Chem. Chem. Phys.*, 2010, **12**, 4275-4286.
- 17 A. Roosjen, H. C. van der Mei, H. J. Busscher and W. Norde, *Langmuir*, 2004, **20**, 10949-10955.
- 18 E. Ostuni, R. G. Chapman, R. E. Holmlin, S. Takayama and G. M. Whitesides, *Langmuir*, 2001, **17**, 5605-5620.
- 19 B. Pidhatika, M. Rodenstein, Y. Chen, E. Rakhmatullina, A. Muhlebach, C. Acikgoz, M. Textor and R. Konradi, *Biointerphases*, 2012, **7**, 1-15.
- 20 C. Crouzet, C. Decker and J. Marchal, *Makromol. Chem.*, 1976, **177**, 145-157.
- 21 F. Kawai, T. Kimura, M. Fukaya, Y. Tani, K. Ogata, T. Ueno and H. Fukami, *Appl. Environ. Microbiol.*, 1978, **35**, 679-684.
- 22 C. F. Gonzalez, W. A. Taber and M. A. Zeitoun, *Appl. Microbiol.*, 1972, **24**, 911-919.
- 23 R. Konradi, B. Pidhatika, A. Muhlebach and M. Textor, *Langmuir*, 2008, **24**, 613-616.
- 24 J. U. Lind, C. Acikgöz, A. E. Daugaard, T. L. Andresen, S. Hvilsted, M. Textor and N. B. Larsen, *Langmuir*, 2012, **28**, 6502-6511.
- 25 B. Pidhatika, J. Iler, V. Vogel and R. Konradi, *Chimia*, 2008, **62**, 264-269.
- 26 B. Pidhatika, J. Möller, E. M. Benetti, R. Konradi, E. Rakhmatullina, A. Mühlebach, R. Zimmermann, C. Werner, V. Vogel and M. Textor, *Biomaterials*, 2010, **31**, 9462-9472.
- 27 H. Wang, L. Li, Q. Tong and M. Yan, *ACS Appl. Mater. Interfaces*, 2011, **3**, 3463-3471.
- 28 H. Wang, J. Ren, A. Hlaing and M. Yan, *J. Colloid Interf. Sci.*, 2011, **354**, 160-167.
- 29 N. Zhang, T. Pompe, I. Amin, R. Luxenhofer, C. Werner and R. Jordan, *Macromol. Biosci.*, 2012, **12**, 926-936.
- 30 N. Zhang, T. Pompe, R. Luxenhofer, C. Werner and R. Jordan, *Polym. Prepr. (Am. Chem. Soc., Div. Polym. Chem.)*, 2012, **53**, 301-302.
- 31 N. Zhang, M. Steenackers, R. Luxenhofer and R. Jordan, *Macromolecules*, 2009, **42**, 5345-5351.
- 32 B. Guillermin, S. Monge, V. Lapinte and J.-J. Robin, *Macromol. Rapid Commun.*, 2012, **33**, 1600-1612.

- 33 L. Tauhardt, K. Kempe, M. Gottschaldt and U. S. Schubert, *Chem. Soc. Rev.*, 2013, **42**, 7998-8011.
- 34 M. Hanford and T. Peeples, *Appl. Biochem. Biotechnol.*, 2002, **97**, 45-62.
- 35 M. Frant, in *Zentrum für Ingenieurwissenschaften Martin-Luther-Universität Halle-Wittenberg*, Halle, 2008.
- 36 M. Frant, P. Stenstad, H. Johnsen, K. Dölling, U. Rothe, R. Schmid and K. Liefelth, *Materialwissenschaft und Werkstofftechnik*, 2006, **37**, 538-545.
- 37 A. Sateesh, J. Vogel, E. Dayss, B. Fricke, K. Dölling and U. Rothe, *J. Biomed. Mater. Res., Part A*, 2008, **84A**, 672-681.
- 38 S. Vidawati, J. Sitterberg, U. Bakowsky and U. Rothe, *Colloids Surf., B*, 2010, **78**, 303-309.
- 39 C. Bücher, X. Grosse, H. Rothe, A. Fiethen, H. Kuhn and K. Liefelth, *Biointerphases*, 2014, **9**, in press.
- 40 J. Piehler, A. Brecht, R. Valiokas, B. Liedberg and G. Gauglitz, *Biosens. Bioelectron.*, 2000, **15**, 473-481.
- 41 M. Hartlieb, D. Pretzel, K. Kempe, C. Fritzsche, R. M. Paulus, M. Gottschaldt and U. S. Schubert, *Soft Matter*, 2013, **9**, 4693-4704.
- 42 C. P. Lin, Y. C. Sung and G. H. Hsiue, *J. Med. Biol. Eng.*, 2012, **32**, 365-372.
- 43 J.-S. Park, Y. Akiyama, F. M. Winnik and K. Kataoka, *Macromolecules*, 2004, **37**, 6786-6792.
- 44 A. Baumgaertel, E. Altuntaş, K. Kempe, A. Crecelius and U. S. Schubert, *J. Polym. Sci., Part A: Polym. Chem.*, 2010, **48**, 5533-5540.
- 45 A. Baumgaertel, C. Weber, N. Fritz, G. Festag, E. Altuntaş, K. Kempe, R. Hoogenboom and U. S. Schubert, *J. Chromatogr. A*, 2011, **1218**, 8370-8378.
- 46 S. Kobayashi, E. Masuda, S. Shoda and Y. Shimano, *Macromolecules*, 1989, **22**, 2878-2884.
- 47 M. Litt, A. Levy and J. Herz, *J. Macromol. Sci., Part A: Pure Appl. Chem.*, 1975, **9**, 703-727.
- 48 A. Levy and M. Litt, *J. Polym. Sci. [A1]: Polym. Chem.*, 1968, **6**, 1883-1894.
- 49 P. Mongondry, C. Bonnans-Plaisance, M. Jean and J. F. Tassin, *Macromol. Rapid Commun.*, 2003, **24**, 681-685.
- 50 M. Agrawal, J. C. Rueda, P. Uhlmann, M. Müller, F. Simon and M. Stamm, *ACS Appl. Mater. Interfaces*, 2012, **4**, 1357-1364.
- 51 C. Bartholome, E. Beyou, E. Bourgeat-Lami, P. Chaumont and N. Zydowicz, *Macromolecules*, 2003, **36**, 7946-7952.
- 52 J. P. Gann and M. Yan, *Langmuir*, 2008, **24**, 5319-5323.